THE JOURNAL OF PHYSICAL CHEMISTRY A

Article

pubs.acs.org/JPCA

# Pressure-Induced Metallization of $Li^+$-Doped Hydrogen Clusters

Ruben Santamaria,* Xim Bokhimi,* and Jacques Soullard*

Instituto de Física, UNAM, A.P. 20-364, México D.F.

Julius Jellinek*

Chemical Sciences and Engineering Division, Argonne National Laboratory, Argonne, Illinois 60439, United States

Supporting Information

**ABSTRACT:** Endohedrally encapsulated hydrogen clusters doped with inert helium ($H_{24}He$) and ionic lithium ($H_{24}Li^+$) are investigated. The confinement model is a nanoscopic analogue of the experimental compression of solid hydrogen. The structural and electronic properties of the doped hydrogen clusters are determined under the effects of pressure. The results are compared with these of the isoelectronic (pure) hydrogen counterpart $H_{26}$ under similar physical conditions. Pressure increase rates with respect to $H_{26}$ of approximately 1.1 are observed with the insertion of helium or lithium. The changes of geometrical structures and HOMO−LUMO gap energies with the pressure point out the pressure-induced metallization of the $Li^+$-doped cluster. The computations are done using density functional theory in the form implemented for molecules; they include zero-point energy effects and, to our best knowledge, are the first of their kind.

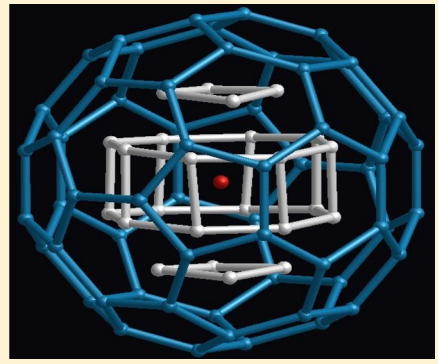

## INTRODUCTION

Hydrogen is the most abundant element in the universe and was predicted to be metallic under high pressure.[1] In this connection, electrical conductivity measurements on solid hydrogen have shown that at room temperature (295 K) and for pressures in the range of 260−270 GPa, the electrical resistance decreases considerably.[2] The compression process used thin layers of Cu and Au as electrodes and an additional thin layer of alumina to create a barrier and block the diffusion of hydrogen into the diamond anvils, avoiding their breaking. Still, the insulator−metal transition was not observed. Other experiments, equally elaborated, have been performed in different forms but without success in finding the metallic state of hydrogen up to 320 GPa.[3] Due to complications in producing mechanically high pressures, the experiments on hydrogen have been limited to a few hundreds GPa; therefore, we face an obstacle to determine its full phase diagram in this direction.

From the theoretical perspective, first-principle methods have played fundamental roles in the search of the metallic state of hydrogen. The method of choice has been density functional theory (DFT), combined with periodic boundary conditions to simulate the extension of the solid and with the inclusion of zero-point vibration (ZPV) energy effects of protons in the harmonic approximation.[4] According to this approach, the closure of an indirect energy band gap (which exhibits dependence on the crystal structure) is predicted to occur at 410 GPa.[5] The calculations have shown the possibility to analyze pressurized hydrogen from a few hundred GPa up to the TPa range.[6] One of the main conclusions is that hydrogen dissociates into a monatomic body-centered tetragonal structure near 500 GPa, with stability up to 1 TPa. At such enormous pressures, the predicted structure is planar hexagonal with a ABC ABC stacking. These studies were restricted to use less than a dozen atoms in the building of the unit cell because the computational cost of the ab initio methods gives little chance to explore alternative arrangements with different numbers of atoms that could lead to other geometries in the conformation of the unit cell. In this regard, similar investigations have been carried out using hydrogen clusters, the finite-size counterpart of crystals,[7−11] and for other systems of energetic interest.[12] In particular, it was shown that hydrogen molecules are capable of self-assemblimg, leading to stable clusters with geometries that depend of both the number of hydrogen molecules and the thermodynamic conditions of pressure and temperature.[9] Some of the important results in this field point out a progressive atomization, starting approximately at 200 GPa, with simultaneous reduction of the energy gap. In short, theoretical calculations indicate that hydrogen in the solid and cluster states demand high pressures to exhibit the expected metallic and atomic phases.

Clearly, one may think of alternative approaches to observe the metallic and atomic phases of hydrogen at lower pressures. One of these considers the insertion of an impurity, in principle capable of modifying the structure and energetics of the clusters. For example, by using $CO_2$ as the second element, it

**Received:** January 15, 2013
**Revised:** May 30, 2013
**Published:** June 12, 2013

   dx.doi.org/10.1021/jp400483z | J. Phys. Chem. A 2013, 117, 5642−5649

was possible to determine the structural and energetic evolution of weakly bounded $He_n$ clusters ($n$ = 1−20).[13,14] In the case of the crystal, the combination of hydrogen with an electropositive element is expected to improve the metallicity.[15−18] The metallic state is rushed up when the second element lowers the gap energy of the insulating phase. Such a possibility has been demonstrated by performing DFT electronic structure calculations of solid hydrogen with lithium.[17] In the pressure range of 100−165 GPa, several phases become metallic and enthalpically stable. Thus, by considering lithium as an impurity, the pressure is reduced, facilitating the process to eventually reach the predicted metallic state.

The goal of the present investigation is to understand the effects of impurities like He and $Li^+$ at the center of an imprisoned 24 H-atom cluster. The number of hydrogen molecules is chosen to follow the isoelectronic series of $H_{26}$, which was the subject of a previous study. We use the thermodynamic model of finite-size systems (TMoFSS) to create the pressure over the cluster and determine the equation of state.[7−11] More precisely, the pressure is applied via volume rescaling of an encapsulating icosahedral hydrogen cage of fullerene-type, $H_{60}$. Like in other studies referent to hydrogen clusters in vacuum[19] and also under compression, we use a similar level of DFT theory to perform the ab initio calculations. The computations account for zero-point energies. Among the main conclusions, we observe that the impurities increase the internal pressure of the cluster, encouraging more ordered structures of the surrounding atoms, and in particular, the cluster with ionic lithium exhibits faster closing of the energy gap by comparing with the other cluster counterparts under similar conditions of pressure.

Finally, molecular clusters and bulk crystals differ in their electronic structure; in the former case, we have discrete energy levels, and in the latter case, we have energy bands. Despite that, the concept of a insulator−metal transition for clusters evolves to the concept used for bulk crystals in the limit of many particles.[20] Therefore, we shall consider that an insulator−metal transition for a cluster occurs when the energy gap is null. The present work takes part in a systematic study on the properties of hydrogen clusters and, in general, of finite-size matter under pressure.

## ■ ENCAPSULATION MODEL AND METHOD

In this work we use the same model of confinement of previous works.[7−11] It consists of a fullerene-type structure composed of 60 hydrogen atoms working as the confining box plus a set of encapsulated hydrogen molecules. The cage can be shrunk and maintained fixed to reproduce different pressures. It has been observed that the action of the pressure leads to the self-assembly of hydrogen molecules into clusters that are energetically and thermodynamically stable, with sizes and geometries that depend not only on the number of imprisoned molecules but also on the pressure. The confinement model has shown to be reliable enough by giving different properties of confined hydrogen clusters in agreement with solid hydrogen under compression and, particularly, has shed light on the atomization and metallization of hydrogen under extreme pressures. The emphasis here is on evaluating the roles of inert helium and ionic lithium (the doping particles) in the structure $H_{24}$. The new structures formed with the insertion of He and $Li^+$ are $H_{24}He$ and $H_{24}Li^+$. We pay attention to their structural and electronic properties by comparing with the isoelectronic and stable cluster $H_{26}$, constituted by hydrogen solely, with the extra $H_2$ particle replacing He and $Li^+$. The expressions that determine the pressure and volume from the basic mechanical variables of position, velocity, and force are discussed briefly; nevertheless, they have been discussed a number of times and can be found elsewhere.[12]

DFT is used to obtain the structural and energy features of the confined isoelectronic clusters $H_{26}$, $H_{24}He$, and $H_{24}Li^+$ in the $H_{60}$ container. The gradient-corrected functionals of Becke for exchange[21] and Lee−Yang−Parr for correlation[22] are used according to the implementation in the NWChem and Gaussian-09 software packages.[23,24] Other exchange−correlation functionals have shown less accurate results with respect to the behavior of the highest occupied molecular orbital−lowest occupied molecular orbital (HOMO−LUMO) gap energy with the pressure.[8] A similar level of theory was applied to investigate the ionic hydrogen clusters $H_3^+(H_2)_n$ in vacuum. The results indicate that molecular hydrogen clusters in vacuum are linked weakly, with dispersive van der Waals forces playing important roles and associated intermolecular bonding energies of just a few Kelvin. The dispersive forces are deficiently described by DFT due to the wrong decay of the energy potential at large distances and the poor description of correlation effects (making also necessary the use of sufficiently large basis sets to avoid basis set superposition errors).[25] In our case, we have the compression of atoms, which minimizes the role played by the van der Waals forces. Also, in relation to the basis sets, it is important to point out here that the number of computations required to determine the ZPV energy of a system with $N$ particles is, in principle, $3N \times 3N$. Such a number corresponds to the dimensions of the Hessian matrix (composed of the second derivatives of the energy with respect to the atomic positions). However, if the off-diagonal part of the Hessian matrix is symmetric ($a_{ij} = a_{ji}$), the number of computations is reduced to $3N(3N + 1)/2$. Thus, even for systems with a relatively small number of particles, the computations grow in quadratic form. In order to compensate for the large number of computations required to obtain the Hessian matrix and determine the zero-point energies of the clusters, we use the moderate basis set 6-31G* because it shows good compromise between accuracy and computational flexibility. Henceforth, the present level of theory imparts some confidence to investigate the clusters of this work.

On the other hand, the one-electron Kohn−Sham equations are iterated until the self-consistent cycles reach convergence thresholds of $10^{-5}$ au in the electron density and energy. The total energy of the cage−cluster system is minimized over the positions of the encapsulated atoms using the quasi-Newton method.[26] The energy minimization thresholds are 0.0015 bohr for the maximum Cartesian step and 0.0015 hartree/bohr for the equilibrium forces. The calculations are carried out for the lowest spin multiplicity. Finally, after performing the energy minimization process, a constrained vibrational frequency analysis of the imprisoned particles is carried out, maintaining the cage atoms fixed at their positions (using the Gaussian software package). This calculation provides the ZPV energy of the confined structure under study. We provide an example of the Gaussian input file as Supporting Information.

## ■ RESULTS

Several calculations of the supermolecule type were performed, and in every case, the structure of the hydrogen cluster was optimized in the hydrogenic cage $H_{60}$, maintaining the cage atoms static for the imposed cage radius $R_c$. The main physical


dx.doi.org/10.1021/jp400483z | J. Phys. Chem. A 2013, 117, 5642−5649

Table 1. Electronic Energies of the Structures $H_{24}He@H_{60}$, $H_{24}Li^+@H_{60}$, and $H_{26}@H_{60}$ and Cage Energy ($H_{60}$)[a]

| $R_c$ | $H_{24}He@H_{60}$ | $H_{24}Li^+@H_{60}$ | $H_{26}@H_{60}$ | $H_{60}$ |
|---|---|---|---|---|
| 2.40 | | −49.5359 (0.2777) | −43.2152 (0.2946) | −32.0941 |
| 2.50 | −45.9776 (0.2652) | −50.4646 (0.2430) | −44.1732 (0.2734) | −32.4834 |
| 2.60 | −46.7344 (0.2627) | −51.1979 (0.2625) | −44.9067 (0.2664) | −32.7644 |
| 2.70 | −47.3196 (0.2685) | −51.7681 (0.2834) | −45.4977 (0.2741) | −32.9602 |
| 2.80 | −47.7773 (0.2744) | −52.2346 (0.2867) | −45.9653 (0.2831) | −33.0844 |
| 2.90 | −48.1400 (0.2687) | −52.6053 (0.2807) | −46.3325 (0.2792) | −33.1501 |
| 3.00 | −48.4108 (0.2613) | −52.8836 (0.2699) | −46.6054 (0.2736) | −33.1681 |

[a]The units of $R_c$ are Å, those of the electronic energy are Hartree, and those of ZPVE (in parentheses) are Hartree.

quantities of interest in the calculations are the spatial structure, total energy $E_{tot}$ (equal to the electronic energy plus ZPV energy, $E_{tot} = E_{elec} + E_{zpv}$), cage energy $E_{H_{60}}$ (with no cluster inside), electronic volume of the confined cluster, together with the gap energy $E_{homo} - E_{lumo}$ of the composed cage−cluster system.

**Energy and Pressure with the Volume.** If we consider a fixed cage radius $R_c$, the energies of the structures $H_{24}He@H_{60}$, $H_{24}Li^+@H_{60}$, and $H_{26}@H_{60}$ are different due to the presence of inert helium, ionic lithium, or $H_2$ at the core of the clusters. Table 1 exhibits the electronic energies of these structures and ZPV energies of the clusters for different cage radii.

The energy per atom of the confined cluster is obtained by subtracting the cage energy from the total energy and dividing by the number $N$ of atoms composing the cluster, $E_{clu} = (E_{tot} - E_{H_{60}})/N$. For instance, for the Li-doped clusters with cage radii of 2.60 and 2.70 Å, we have the energies per atom of −0.7268 and −0.7410 au, respectively. Interestingly, if we use the larger basis set 6-31G** in the calculations, the corresponding energies are −0.7341 and −0.7486 au. The relative energy in the first case is −0.0142 au, and that in the second case is −0.0145 au. In this regard, the basis sets 6-31G* and 6-31G** provide essentially the same result.

The volume $V$ of confinement corresponds to the electronic volume per atom of the confined cluster. It is computed in the form $V = (4\pi/3)R_{conf}^3/N$, with $R_{conf} = R_{clu} + (R_c - R_{clu})/2$, where the quantity $R_{clu}$ is the cluster radius. The term $(R_c - R_{clu})/2$ is the contribution of the electron cloud to the confining radius. Table 2 gives the cage radius and confinement radius of each structure.

The set of energies $E_{clu}$ with the corresponding confinement volumes are portrayed in the first inset of Figure 1 with filled circles. We have parametrized the data $E_{clu}$ versus $V$ (in atomic units) with an expression of the type

$$E_{clu}(V) = a + be^{\alpha V^{1/3}} + cV^{1/3}e^{\alpha V^{1/3}}$$

The parametrization lets us manipulate the data analytically, for instance, for the computation of the pressure. The set of parameters $(a, b, c, \alpha)$ for $H_{24}He$ are (−0.658921, 11.0543, 0.0345819, −2.15142), for $H_{24}Li^+$, we have (−0.826997, −65.6111, 72.7757, −3.16335), and for $H_{26}$, they are (−0.546662, −532.135, 409.019, −3.8778). The parametrizations are depicted with lines in the first inset of Figure 1. Once the parameters for every structure are determined, the static pressure is obtained by differentiation of the cluster energy in the form $P = -\partial E_{clu}/\partial V$.

$$P = -\frac{\partial E_{clu}}{\partial V} = -\left(\frac{\alpha b}{3V^{2/3}} + \frac{\alpha c}{3V^{1/3}} + \frac{c}{3V^{2/3}}\right)e^{\alpha V^{1/3}}$$

The curve $PV$ is the equation of state in the zero-temperature approximation. It is shown in the second inset of Figure 1 for every cluster (with ZPV energies included). The overall observations of Figure 1 follow: the energies and pressures of the confined clusters $H_{24}He$, $H_{24}Li^+$, and $H_{26}$ present decaying behavior when the volume increases. The energies of the doped clusters are more negative than those of the pure hydrogen cluster. In the case of the pressure, the previous behavior is reversed because the pressure of the cluster $H_{26}$ is always lower than those of $H_{24}He$ and $H_{24}Li^+$ for equal cage radii (refer to the second inset of Figure 1). However, the pressures of $H_{24}He$ and $H_{24}Li^+$ are very similar and only differ at very low or very high pressures. Therefore, the replacement of the central hydrogen molecule $H_2$ in $H_{26}$ by He or $Li^+$ lowers the energy but increases the pressure. The pressure rate increase in going from the system $H_{26}$ to $H_{24}He$ or $H_{24}Li^+$, for the same cage radius, is approximately a factor of 1.1. More precisely, if the pressure associated with $H_{26}$ and observed at a given volume is multiplied by a factor of 1.1, then the pressure of $H_{24}Li^+$ or $H_{24}He$ is closely reproduced for such a volume. In this regard, the factor 1.1 summarizes the roles that He and $Li^+$ play in increasing the pressure and for the specific particle densities used in this work. On the other hand, we do not observe any regular pattern of the ZPV energies with the pressure. Moreover, when the calculations are performed with and without ZPV effects, small differences (of less than a 12 GPa) are observed in the pressure.

The pressure (in GPa) of the confined cluster $H_{26}$ is shown with the volume (in $cm^3$/mole) in Figure 2. We report the Vinet fit of experimental measurements of Hemley et al.,[27−29] together with the fit of Evans and Silvera[30] in the same figure for comparison purposes. Despite the fact that we deal with a cluster, the results of $H_{26}$ are in fair agreement with experimental measurements on the solid. In this regard, the main properties that define the equation of state are largely of local character.

Table 2. Cage Radius $R_c$ and Confinement Radius $R_{conf}$ of the Structures $H_{24}He@H_{60}$, $H_{24}Li^+@H_{60}$, and $H_{26}@H_{60}$[a]

| | $R_{conf}$ | | |
|---|---|---|---|
| $R_c$ | $H_{24}He@H_{60}$ | $H_{24}Li^+@H_{60}$ | $H_{26}@H_{60}$ |
| 2.40 | | 1.927 | 1.920 |
| 2.50 | 1.986 | 2.006 | 1.996 |
| 2.60 | 2.057 | 2.061 | 2.062 |
| 2.70 | 2.124 | 2.129 | 2.128 |
| 2.80 | 2.190 | 2.199 | 2.193 |
| 2.90 | 2.262 | 2.272 | 2.265 |
| 3.00 | 2.333 | 2.344 | 2.337 |

[a]The units of $R_c$ and $R_{conf}$ are Å.


dx.doi.org/10.1021/jp400483z | J. Phys. Chem. A 2013, 117, 5642−5649

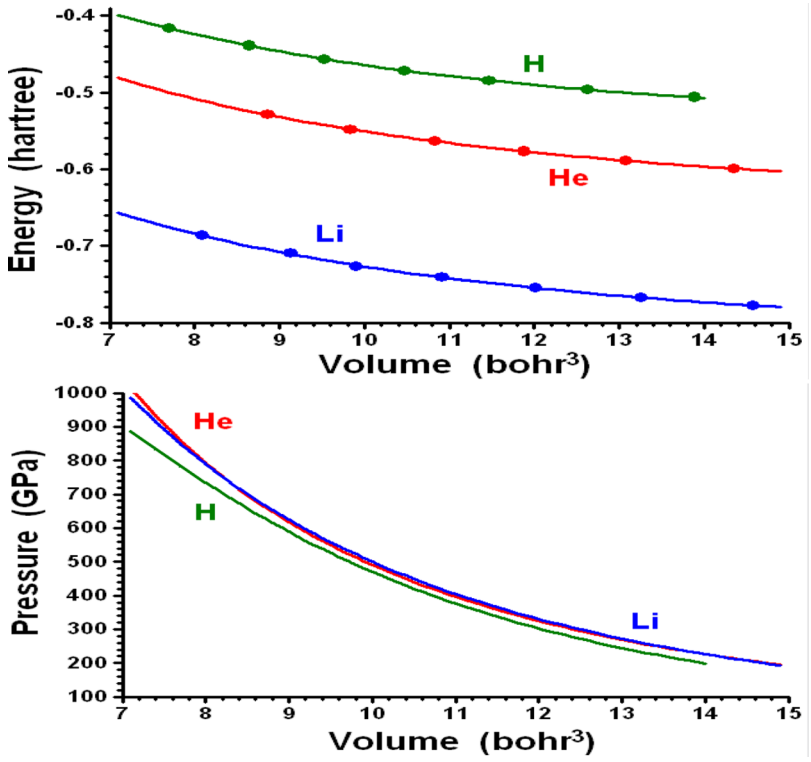


**Figure 1.** The energies and pressures per atom of the confined isoelectronic clusters $H_{24}He$ (red lines), $H_{24}Li^+$ (blue lines), and $H_{26}$ (olive lines) are shown with the volume per atom. The filled circles in the first inset correspond to the numerical results, while the curves represent fitting lines.

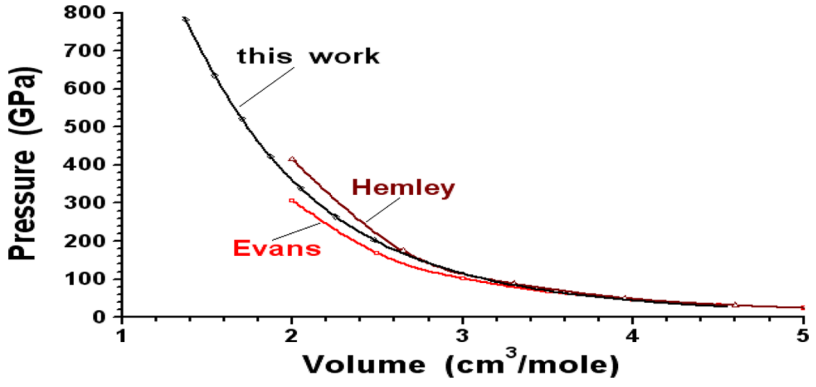


**Figure 2.** The pressure of the confined cluster $H_{26}$ (black line with open diamonds) is shown with the volume. The other lines in color and with symbols are experimental measurements of Hemley[27−29] (brown △) and Evans[30] (red □). The experimental data were extrapolated to high pressures by us for comparison purposes solely.

It is important to investigate the electronic coupling of the encased cluster atoms with the atoms of the cage because, in this way, it is possible to measure the changes exerted by the "environment" on the cluster. The coupling effect is estimated by comparing the electronic energy per atom of the *free* cluster at the geometry imposed by the confining cage, say $E'_{clu}$, with the electronic energy of the imprisoned cluster $E_{clu} = (E_{tot} - E_{H_{60}})/N$ (previously discussed and illustrated in the first inset of Figure 1). Table 3 gives the electronic coupling $E'_{clu} - E_{clu}$ for the different sets of clusters and cage radii.

The first observation in this regard is that clusters without cage borders give lower electronic energies than the clusters with cage borders due to the relaxation of the electron clouds. As expected, the electronic coupling of the cluster with the container increases when the radius of the spherical container diminishes. The coupling is approximately similar for the different types of clusters because they all have similar external compositions (it is the inner part compositions that are really different). Note that the coupling is unavoidable, physically

**Table 3. Electronic Coupling Per Atom of the Cluster with the Confining Cage[a]**

| $R_c$ | $H_{24}He$ | $H_{24}Li^+$ | $H_{26}$ |
|---|---|---|---|
| 2.40 | | −0.0691 | −0.0737 |
| 2.50 | −0.0686 | −0.0568 | −0.0605 |
| 2.60 | −0.0598 | −0.0538 | −0.0578 |
| 2.70 | −0.0530 | −0.0540 | −0.0497 |
| 2.80 | −0.0457 | −0.0467 | −0.0444 |
| 2.90 | −0.0397 | −0.0402 | −0.0389 |
| 3.00 | −0.0345 | −0.0346 | −0.0389 |

[a]The units of $R_c$ are Å, and those of the electronic energy are Hartree.


dx.doi.org/10.1021/jp400483z | J. Phys. Chem. A 2013, 117, 5642−5649

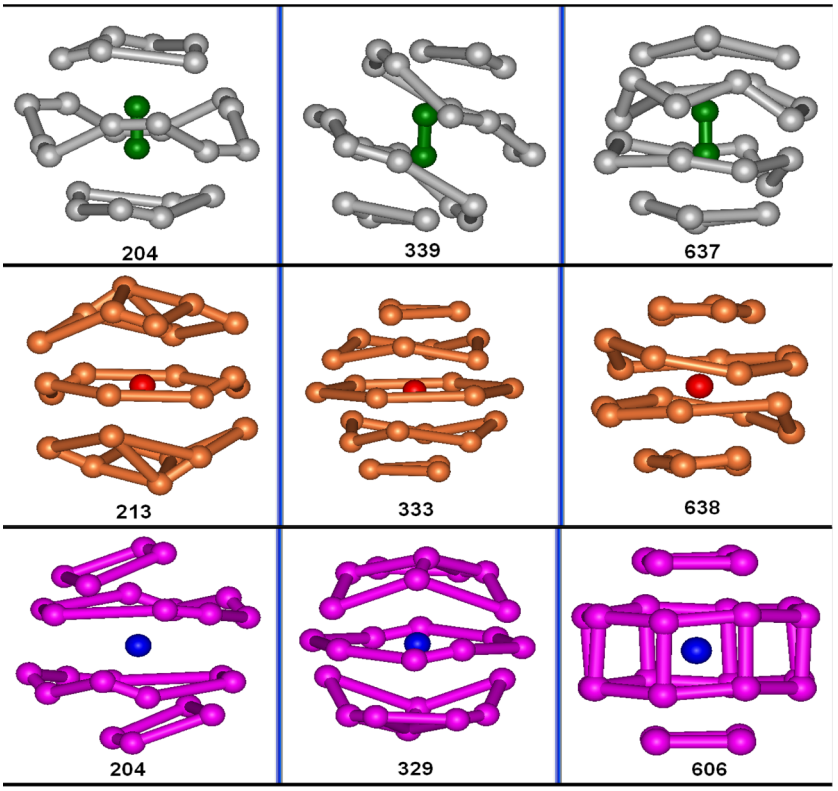


**Figure 3.** The energetically optimized structures of the confined isoelectronic clusters $H_{26}$ (first row), $H_{24}He$ (second row), and $H_{24}Li^+$ (third row) are presented for some selected pressures (indicated below each inset in GPa units). The cluster structures change with the pressure (from left to right) and the doping element (from top to bottom).

acceptable, and substantial for finite-size systems that are compressed by walls with atomic structure. Thus, the approach presented here to measure the electronic coupling is of general nature.

**Geometrical Structures.** The pressure exerted over the isoelectronic clusters produces different atom distributions; some of these are shown in Figure 3. The structures evolve toward more ordered ones by increasing the pressure (refer to the structures from left to right in Figure 3). The doping particles appear intercalated between planes for some pressures and in the planes for others. The clusters with $H_2$ at the center are the most disordered structures; the disorder persists up to high pressure rates (this was also observed in ref 11). On the other hand, the presence of helium and lithium at the cores of the hydrogen clusters imposes more order to the structures (this result is also found in free Li-doped $H_2$ clusters[31]). In our case, the structure with higher order is that containing ionic lithium at 606 GPa; still, none of them has perfect symmetry. In order to illustrate the degree of symmetry of this cluster, let us compare its morphology with that of a 24-particle structure with exact orthorhombic ($D_{2h}$) symmetry. The morphologies of the cluster and $D_{2h}$ structure are quite similar; each of them consists of an orthorhombic cell (with 8 external atoms) perpendicular to the horizontal faces of a prism with octagonal symmetry. In the case of the Li-doped cluster at 606 GPa, the average distance of in-plane atoms is close to 1 Å but with some irregularities. In contrast, the in-plane interatomic distances of the $D_{2h}$ structure are repeated exactly (we believe that these interatomic distances correspond to the first peak of the last plot of Figure 5, while the second peak there is associated with atom pairs belonging to different planes). The conclusion is that none of the confined clusters exhibit perfect symmetry due to irregular interatomic distances.

At high pressures, the atoms get too close to each other, in such a way that the bond with an exclusive partner fades out because other partners appear equally close. This represents the atomization state of the hydrogen clusters (such an observation is consistent with those deduced in refs 8 and 9). The atomization state is also characterized by highly symmetric structures (additional discussion comes later by analyzing pair distribution functions, (PDFs).

**HOMO–LUMO Gap Energy.** It is important to examine the HOMO–LUMO gap energy behavior of the structures with the pressure; they are provided in Table 4. The HOMO–LUMO gap energy is characteristic of the whole cluster plus cage atoms, and therefore, care should be exercised in the interpretation associated with the confined clusters. To do this,

**Table 4. Variation of the HOMO–LUMO Gap Energy of the Isoelectronic Structures $H_{26}@H_{60}$, $H_{24}He@H_{60}$, and $H_{24}Li^+@H_{60}$ and Empty Cage $H_{60}$ with the Pressure[a]**

| | $H_{26}@H_{60}$ | | $H_{24}He@H_{60}$ | | $H_{24}Li^+@H_{60}$ | | $H_{60}$ |
|---|---|---|---|---|---|---|---|
| $R_c$ | pressure | gap | pressure | gap | pressure | gap | gap |
| 3.00 | 204 | 1.01 | 213 | 1.02 | 204 | 1.29 | 2.031 |
| 2.90 | 264 | 0.94 | 266 | 0.93 | 260 | 1.16 | 2.133 |
| 2.80 | 339 | 0.84 | 333 | 0.84 | 329 | 1.01 | 2.242 |
| 2.70 | 422 | 0.86 | 410 | 0.85 | 412 | 1.06 | 2.359 |
| 2.60 | 522 | 0.72 | 508 | 0.75 | 511 | 0.21 | 2.486 |
| 2.50 | 637 | 1.98 | 638 | 0.72 | 606 | 2.28 | 2.616 |
| 2.40 | 784 | 2.02 | | | 773 | 2.31 | 2.765 |

[a]The pressure is in GPa, and the energy is in eV.


dx.doi.org/10.1021/jp400483z | J. Phys. Chem. A 2013, 117, 5642–5649

we have inserted in the last column of Table 4 the gap energy of the empty cages.

The gap energy of the empty cages increases monotonically when the cage radius decreases. In this regard, any change of such a behavior for the investigated structures may be attributed to the clusters inside the cages. The gap energy of the clusters inside the cages shows decreasing behavior up to ∼510 GPa (for helium, the decreasing behavior goes beyond 510 GPa). In none of these cases is the gap energy completely closed. A study performed by Somayazulu et al.[32] (motivated by the Carlsson−Ashcroft work referent to doping effects[15]) on solid hydrogen doped with inert Xe, under a pressure of 240 GPa, found no metallization on such structures. In our case, the cluster doped with ionic lithium at 511 GPa is the one that achieves major closing (of just 0.21 eV). This closing process starts slowly and in a progressive manner at moderate pressures, but at high pressures, it is abrupt, pointing out to a metallic state. At pressures higher than 520 GPa, the decreasing behaviors of the gap energies of the hydrogen and lithium clusters are reversed and start to increase (except for the cluster with helium, for which, nevertheless, a similar behavior is expected at higher pressures). Such a behavior is due to a significant influence of the cages on the electronic structure of the clusters. Therefore, in this very high pressure domain, we confirm that the borders strongly interact with the encapsulated atoms (as initially noted in terms of the electron coupling in a previous section).

In Figure 4, the HOMO orbital density of the system $H_{24}Li^{+}@H_{60}$, with a cage radius of 2.50 Å, is depicted. The

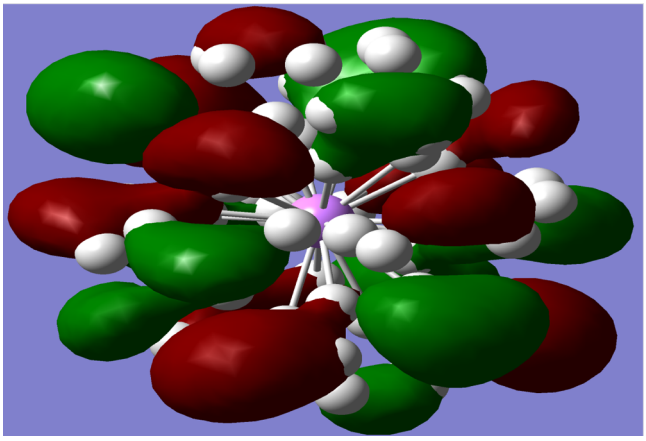

**Figure 4.** The density of the HOMO of the system $H_{24}Li^{+}@H_{60}$, cage radius of 2.50 Å, is exhibited. The HOMO electron density is distributed symmetrically over the cluster and spherical container. The different colors correspond to spin-up and spin-down electron densities.

HOMO density is a property of the whole system, and it is found to be distributed over the whole region of the cluster and container. For a smaller cage radius (inducing higher pressure on the imprisoned cluster), the electronic coupling between the cluster and container is large enough (refer to Table 3), and the HOMO−LUMO gap is dominated by the whole system rather than the cluster itself. In other words, at very high pressures, the atoms exerting the confinement have strong influence on the gap energy of the imprisoned clusters, and in this pressure regime, the cage and imprisoned particles are strongly coupled, essentially forming a single entity, and it is not possible to individualize the discussion on the cluster. The conclusion to this section is that clusters containing ionic lithium show faster closing of the energy gap by comparing with their $H_{26}$ and $H_{24}He$ isoelectronic counterparts. In this regard, the $H_{24}Li^{+}$ clusters are expected to achieve metallization at a lower pressure than the other isoelectronic clusters.

**PDF.** In order to appreciate the spatial distribution of atoms in the clusters, the PDF was calculated. The evolution of the PDF with the pressure is depicted in Figure 5.

The distribution function of $H_{26}$ follows similar patterns to those of $H_{24}$ published in a previous work.[9] At low pressure (around 200 GPa), the distribution function of the hydrogen cluster $H_{26}$ presents two main branches. The first branch appears approximately centered at $r$ = 0.725 Å. In essence, this is the bond distance of $H_2$ in vacuum. The second branch, with small shoulders, points out the relative large separation distances between pairs of atoms that belong to different molecules. When the pressure increases to 339 GPa, the heights of the two branches are reduced, both getting slightly wider, and the second branch gets closer to the first one. It is at a pressure of ∼637 GPa that the two branches merge into a single one that is smaller and wider, almost conforming a uniform PDF (or plateau). In this last case, the intramolecular distances increase (making the initial bond distances of 0.725 Å fade out). It indicates an atomization state of the individual $H_2$ molecules. The pressure-induced behavior of the distribution function of $H_{24}He$ is similar to that of $H_{26}$. In this case, the bimodal distribution function merges into a single branch at around 638 GPa; nevertheless, we do not observe a clear plateau this time. Apparently, we require further pressure to observe a uniform PDF.

The PDF of the doped cluster $H_{24}Li^{+}$ is shown in the last inset of Figure 5. At low pressure (∼204 GPa), there are two significant branches indicative of spatial order. The branches are located at distances slightly larger than those observed on the previous clusters. Like in the previous situations, the branches appear closer to each other when the pressure is 329 GPa. This behavior is due to the fact that molecules move closer with the pressure, with the intermolecular and intrapair distances becoming similar (in this case, the intermolecular interactions, once considered weak interactions at low pressures, gradually become stronger[9]). However, contrary to the previous observations, we have a bimodal PDF at 606 GPa. The two branches are well-defined and sufficiently close to each other, indicating spatial order. In this regime, the initial molecular bond distances measured at low pressures are enlarged, showing the atomization state of the cluster. In this sense, the lithium impurity additionally facilitates the atomization of the hydrogen molecules.

Interestingly, large hydrogen structures doped with helium and lithium, and probably nanostructures too, may play important roles in the inner regions of very large objects such as the Jovian planets. It is known that Neptune and Uranus have smaller sizes than Saturn; yet, their mass densities are higher than Saturn's density. In turn, Saturn and Jupiter are close in size, but Jupiter exhibits twice the mass density of Saturn.[33] In this work, we have shown that for similar volumes of pure hydrogen and hydrogen with lithium, different pressures are obtained. Therefore, under the supposition of similar cores of the Jovian planets (a statement generally accepted), a difference in the amounts of doping elements of the hydrogen structures in the outer layers of the cores may be one among other possible factors responsible for the different sizes and densities of the Jovian planets. Lastly, hydrogen


dx.doi.org/10.1021/jp400483z | J. Phys. Chem. A 2013, 117, 5642−5649

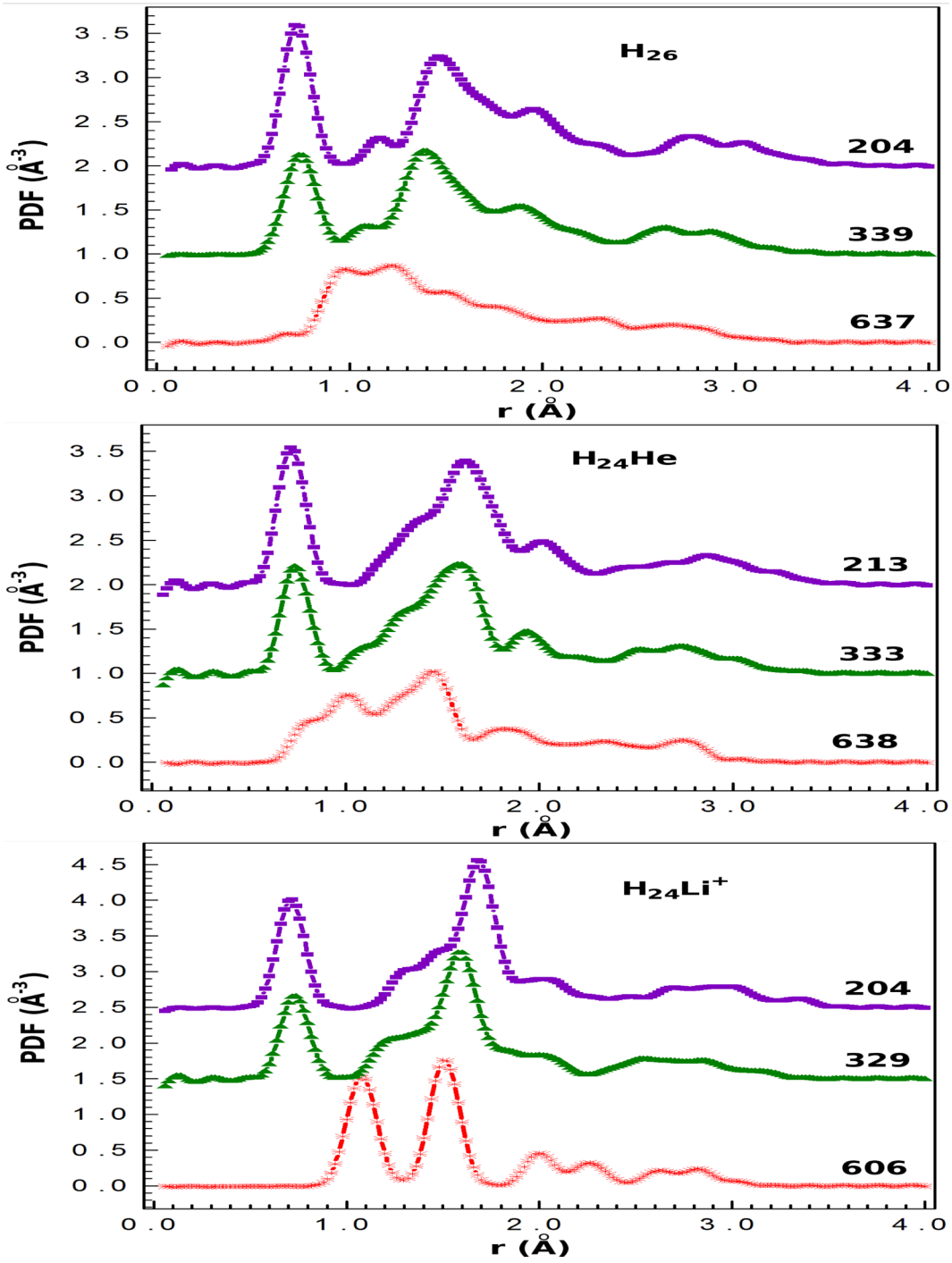


**Figure 5.** The PDFs per volume of the $H_{26}$, $H_{24}He$, and $H_{24}Li^+$ clusters are presented with the pressure (in GPa). All of the PDFs depart from the zero base line, but a depth cue is used to facilitate the visualization. The geometrical structures corresponding to the PDFs are those of Figure 3.

structures doped with helium and lithium are expected to be also of help in the investigation of hydrogen storage technology.

## CONCLUSIONS

We have investigated the roles played by inert and ionic impurities in the structural and electronic properties of hydrogen clusters subject to pressure effects. By comparing the doped clusters $H_{24}He$ and $H_{24}Li^+$ with the pure hydrogen cluster $H_{26}$, differences in the energy and equation of state were determined. For similar confinement volumes of $H_{24}He$, $H_{24}Li^+$, and $H_{26}$, the presence of helium and lithium in the cores of the clusters increases the pressure. The estimated increase rate is approximately 10%. The cluster structures containing helium and lithium evolve toward more ordered structures by increasing the pressure. Yet, lithium is the element that imparts higher spatial order to the surrounding atoms.

At pressures of the order of 600 GPa, the encapsulated atoms show neighborhood atoms at similar distances, indicative of an atomization state. This state is characterized by a structure consisting of hydrogen atoms with high spatial order. The PDF confirms this observation by showing atoms making pairs with


dx.doi.org/10.1021/jp400483z | J. Phys. Chem. A 2013, 117, 5642−5649

several other neighboring atoms (in other words, preferential partners fade out). On the other hand, the HOMO−LUMO gap energies of $H_{26}$, $H_{24}He$, and $H_{24}Li^+$ diminish by increasing the pressure. For moderate pressures, the closing of the gap proceeds very slowly, in such a way that the atomization state is achieved before the complete closing of the HOMO−LUMO gap energy. However, at high pressures, the gap energy of the cluster containing ionic lithium is abruptly reduced, reaching a value of 0.21 eV at around 511 GPa. Therefore, there is a pressure domain where the metallization may be achieved faster by doping hydrogen with lithium.

## ■ ASSOCIATED CONTENT

### Supporting Information

Gaussian input for the Li-doped hydrogen cluster inside of the hydrogenic fullerene cage. This material is available free of charge via the Internet at http://pubs.acs.org.

## ■ AUTHOR INFORMATION

### Corresponding Author

*E-mail: rso@fisica.unam.mx (R.S.); bokhimi@fisica.unam.mx (X.B.); soullard@fisica.unam.mx (J.S.); jellinek@anl.gov (J.J.).

### Notes

The authors declare no competing financial interest.

## ■ ACKNOWLEDGMENTS

The authors thank the *IFUNAM* and *DGTIC* computer staff for access to Khua and KanBalam CPU clusters. J.J. was supported by the Office of Basic Energy Sciences, Division of Chemical Sciences, Geosciences, and Biosciences, U.S. Department of Energy under Contract No. DE-AC02-06CH11357. We thank Dr. J. M. Lopez-Encarnacion for help with input files for constrained normal mode calculations.

## ■ REFERENCES

(1) Wigner, E. P; Huntington, H. B. On the Possibility of a Metallic Modification of Hydrogen. *J. Chem. Phys.* **1935**, *3*, 764−770.
(2) Eremets, M. I.; Troyan, I. A. Conductive Dense Hydrogen. *Nat. Mater.* **2011**, *10*, 927−931.
(3) Loubeyre, P.; Occelli, F.; Le Toullec, R. Optical Studies of Solid Hydrogen to 320 GPa and Evidence for Black Hydrogen. *Nature* **2002**, *416*, 613−617.
(4) Pickard, C. J.; Needs, R. J. Structure of Phase III of Solid Hydrogen. *Nat. Phys.* **2007**, *3*, 473−476.
(5) Johnson, K. A.; Ashcroft, N. W. Structure and Bandgap Closure in Dense Hydrogen. *Nature* **2000**, *403*, 632−635.
(6) McMahon, J. M.; Ceperley, D. M. Ground-State Structures of Atomic Metallic Hydrogen. *Phys. Rev. Lett.* **2011**, *106*, 165302.
(7) Soullard, J.; Santamaria, R.; Cruz, S. Endohedral Confinement of Molecular Hydrogen. *Chem. Phys. Lett.* **2004**, *391*, 187−190.
(8) Santamaria, R.; Soullard, J. The Atomization Process of Endohedrally Confined Hydrogen Molecules. *Chem. Phys. Lett.* **2005**, *414*, 483−488.
(9) Soullard, J.; Santamaria, R.; Jellinek, J. Pressure and Size Effects in Endohedrally Confined Hydrogen Clusters. *J. Chem. Phys.* **2008**, *128*, 064316.
(10) Santamaria, R.; Soullard, J.; Jellinek, J. Thermal Behavior of a 13-Molecule Hydrogen Cluster under Pressure. *J. Chem. Phys.* **2010**, *132*, 124505.
(11) Soullard, J.; Santamaria, R.; Boyer, D. Thermodynamic States of Nanoclusters at Low Pressure and Low Temperature: The Case of $13H_2$. *J. Phys. Chem. A* **2011**, *115*, 9790−9800.
(12) Santamaria, R.; Mondragón-Sánchez, J. A.; Bokhimi, X. Equation of State of a Model Methane Clathrate Cage. *J. Phys. Chem. A* **2012**, *116*, 3673−3680.
(13) Ing, C.; Hinsen, K.; Yang, J.; Zeng, T.; Li, H.; Roy, P.-N. A Path-Integral Langevin Equation Treatment of Low-Temperature Doped Helium Clusters. *J. Chem. Phys.* **2012**, *136*, 224309.
(14) Li, H.; Blinov, N.; Roy, P.-N.; Le Roy, R. J. Path-Integral Monte Carlo Simulation of V3-Vibrational Shifts for $CO_2$ in $(He)_n$ Clusters Critically Tests the He−$CO_2$ Potential Energy Surface. *J. Chem. Phys.* **2009**, *130*, 144305.
(15) Carlsson, A. E.; Ashcroft, N. W. Approaches for Reducing the Insulator−Metal Transition Pressure in Hydrogen. *Phys. Rev. Lett.* **1983**, *50*, 1305−1308.
(16) Ashcroft, N. W. Hydrogen Dominant Metallic Alloys: High Temperature Superconductors? *Phys. Rev. Lett.* **2004**, *92*, 187002.
(17) Zurek, E.; Hoffmann, R.; Ashcroft, N. W.; Oganov, A. R.; Lyakhov, A. O. A Little Bit of Lithium Does a Lot for Hydrogen. *Proc. Natl. Acad. Sci. U.S.A.* **2009**, *106*, 17640−17643.
(18) Yao, Y.; Klug, D. D. Silane Plus Molecular Hydrogen As a Possible Pathway to Metallic Hydrogen. *Proc. Natl. Acad. Sci. U.S.A.* **2010**, *107*, 20893−20898.
(19) Huang, L.; Matta, C. F.; Massa, L. Ion Induced Dipole Clusters $H_n^-$ ($3 \leq n -$ odd $\leq 13$): Density Functional Theory Calculations of Structure and Energy. *J. Phys. Chem. A* **2011**, *115*, 12445−12450.
(20) Mott, N. F. *Metal−Insulator Transition*; Taylor and Francis: London, 1990, p 124.
(21) Becke, A. D. Density-Functional Exchange-Energy Approximation with Correct Asymptotic Behavior. *Phys. Rev. A* **1988**, *38*, 3098−3100.
(22) Lee, C.; Yang, W.; Parr, R. G. Development of the Colle−Salvetti Correlation Energy Formula into a Functional of the Electron Density. *Phys. Rev. B* **1988**, *37*, 785−789.
(23) Valiev, M.; Bylaska, E. J.; Govind, N.; Kowalski, K.; Straatsma, T. P.; van Dam, H. J. J.; Wang, D.; Nieplocha, J.; Apra, E.; Windus, T. L.; de Jong, W. A. NWChem: A Comprehensive and Scalable Open-Source Solution for Large Scale Molecular Simulations. *Comput. Phys. Commun.* **2010**, *181*, 1477−1489.
(24) Frisch, M. J.; Trucks, G. W.; Schlegel, H. B.; Scuseria, G. E.; Robb, M. A.; Cheeseman, J. R.; Scalmani, G.; Barone, V.; Mennucci, B.; et al. *Gaussian 09*, revision A.02; Gaussian, Inc.: Wallingford, CT, 2009.
(25) Bokes, P.; Štich, I.; Mitas, L. Electron Correlation Effects in Ionic Hydrogen Clusters. *Int. J. Quantum Chem.* **2001**, *83*, 86−95.
(26) Nocedal, J.; Wright, S. J. *Numerical Optimization*; Springer: New York, 1999; Chapters 8 and 9.
(27) Hemley, R. J.; Mao, H. K.; Finger, L. W.; Jephcoat, A. P.; Hazen, R. M.; Zha, C. S. Equation of State of Solid Hydrogen and Deuterium from Single-Crystal X-ray Diffraction to 26.5 GPa. *Phys. Rev. B* **1990**, *42*, 6458−6470 ; see eq 7.
(28) Loubeyre, P.; Le Toullec, R.; Hausermann, D.; Hanfland, M.; Hemley, R. J.; Mao, H. K.; Finger, L. W. X-ray Diffraction and Equation of State of Hydrogen at Megabar Pressures. *Nature* **1996**, *383*, 702−704.
(29) Hemley, R. J.; Mao, H. K. Progress in Cryocrystals at Megabar Pressures. *J. Low Temp. Phys.* **2001**, *122*, 331−344.
(30) Evans, W. J.; Silvera, I. F. Index of Refraction, Polarizability, and Equation of State of Solid Molecular Hydrogen. *Phys. Rev. B* **1998**, *57*, 14105−14109 ; see eq 7.
(31) Scharf, D.; Martyna, G. J.; Klein, M. L. Path-Integral Monte Carlo Study of a Lithium Impurity in para-Hydrogen: Clusters and the Bulk Liquid. *J. Chem. Phys.* **1993**, *99*, 8997−9012.
(32) Somayazulu, M.; Dera, P.; Goncharov, A. F.; Gramsch, S. A.; Liermann, P.; Yang, W.; Liu, Z.; Mao, H.; Hemley, R. J. Pressure-Induced Bonding and Compound Formation in Xenon−Hydrogen Solids. *Nat. Chem.* **2010**, *2*, 50−53.
(33) *The Outer Planets*. http://lasp.colorado.edu/education/outerplanets/giantplanets_interiors.php (2007).